

NON-LINEAR ANALYSIS OF PLATED T-SUBJECTED TO NEGATIVE BENDING MOMENT

Ahmed Abdullah Mansor

Engineering Collage / Diyala University

(Received:15/4/2012 ; Accepted:26/6/2012)

ABSTRACT:- This paper present a numerical analysis using ANSYS finite element program to simulate the reinforced concrete T- beams strengthened with external bonded steel plates when subjected to negative bending. Eight beams with length 2.0m and simply supported were modeled. Nonlinear materials behavior, as it relates to steel reinforcing bars and plain concrete, and linear behavior for plate is simulated using appropriate constitutive models. The results showed that the general behavior of the finite element models represented by the load-deflection curves at midspan appear well agreement with the test data from the previous researches. Also the crack patterns at the final loads from the finite models are discussed . The finite element models represented by this search can be used to carry out parametric study for the strengthening of plated T-beams.

Keyword: Finite Element Modeling; Reinforced Concrete Beams; Strengthened T-beam, Plate, Epoxy Resin.

1. INTRODUCTION

In recent years, the development of a wide variety of epoxy adhesive, has given rise to new technique for repairing and strengthening concrete structures. These techniques include gluing steel plates to the surface of the concrete. The overall aim of the present experimental work was to study strength and deformation characteristics of R/C T-beam strengthened with steel plates glued to their tension faces when subjected to the negative bending moment. The test therefore, simulate the hogging moment region of the continuous beam or inverted T-beam. The main parameters investigated were as mention above.

In this paper, A theoretical analysis to predict the flexural (deflection, cracking load and ultimate load) of both strengthened and conventional R/C beams was performed, using a nonlinear finite element ANSYS 12 program⁽¹⁾ based on the eight full scale reinforce concrete beam tested⁽²⁾.

2. DETAILS OF EXPERIMENTAL TEST⁽²⁾

2.1 OUT LINE OF PROGRAM

Eight beams were tested, full details of their dimensions, arrangement of reinforcing steel and loading set up are shown in Fig.1 and variables studied are given in Table1. For all strengthened beams, the glue layer thickness was constant at 1.5mm and the steel plates were stopped 5 cm short of supports. Four thickness 1, 2, 3 and 4 mm of mild steel plates with yield strengths 260, 310, 208 and 246N/mm² respectively were used as strengthening reinforcement. Epoxy compound was used as adhesive material in this work. Compressive, bending and adhesive strength on concrete of Epoxy adhesive as given by the manufacturers are 6000, 2500 and 250 N/mm² respectively.

2.2 TESTED METHOD AND MEASUREMENT

All beams were tested under simply supported condition over a span 2.0m with their tension faces uppermost as shown in Fig.1. for all beams, the first crack load, deflection under loading point, steel plate strains and ultimate load were measured.

3. MATERIAL PROPERTIES AND CONSTITIVE MODELS

3.1 ELEMENT TYPE

An eight-node solid element, Solid65, was used to model the concrete. The solid element has eight nodes with three degrees of freedom at each node-translations in the nodal x, y and z directions. The element is capable of plastic deformation, cracking in three orthogonal directions, and crushing. The geometry and node locations for the element type are shown in Fig.2

A Link 8 was used to model the steel reinforcement. Two nodes are required for this element. Each node has three degree of freedom, at each node-translations in threenodal x, y and z directions. The element is also capable of plastic deformation. The geometry and node locations for this element type are shown in Fig. 3.

An eight-node solid element, Shell43, was used for the steel plates as strengthening reinforcement. The geometry and node locations for the element type are shown in Fig.4.

An eight-node solid element, Solid45, was used for the steel plates at the supports and applied load location in the beam models. The element is defined with eight nodes having three degrees of freedom at each node-translations in the nodal x, y and z directions. The geometry and node locations for the element type are shown in Fig.5.

3.2 MODELING of MATERIAL PROPERTIES

3.2.1 Concrete

In compression, the stress-strain curve for concrete is linearly elastic up to about 30 percent of the maximum compressive strength. Above this point, the stress increases gradually up to the maximum compressive strength. After it reaches the maximum compressive strength σ_{cu} , the curve descends into a softening region, and eventually crushing failure occurs at an ultimate strain ϵ_{cu} . In tension, the stress-strain curve for concrete is approximately linearly elastic up to the maximum tensile strength. After this point, the concrete cracks and the strength decreases gradually to zero. Fig.6 shows typical uniaxial compressive and tensile stress-strain curve for concrete.

The present study assumed that the concrete is a homogenous and initially isotropic. The compressive uniaxial stress-strain relationship for concrete model is obtained by using the following equations which can be used to compute the multilinear isotropic stress-strain curve for the concrete^{(3),(4)} is as shown in Fig. 7⁽⁵⁾.

$$f_c = \epsilon E_c \quad \text{for } 0 \leq \epsilon \leq \epsilon_1 \quad \dots\dots\dots(1)$$

$$f_c = \frac{\epsilon E_c}{1 + \left[\frac{\epsilon}{\epsilon_0}\right]^2} \quad \text{for } \epsilon_1 \leq \epsilon \leq \epsilon_0 \quad \dots\dots\dots(2)$$

$$f_c = f_c' \quad \text{for } \epsilon_0 \leq \epsilon \leq \epsilon_{cu} \quad \dots\dots\dots(3)$$

$$\epsilon_0 = \frac{2 f_c'}{E_c} \quad \text{for } \epsilon_0 \leq \epsilon \leq \epsilon_{cu} \quad \dots\dots\dots(4)$$

The simplified stress-strain curve for each beam model is constructed from six points connected by straight lines. The curve starts at zero stress and strain. Point 1, at $0.3f_c'$, is calculated for stress-strain relationship of the concrete in the linear range(must satisfy Hooke's law). Point 5 is at ϵ_0 and f_c' . The behavior is assumed to be perfectly plastic after point 5⁽⁶⁾.

3.2.2 Steel

Steel was assumed to be an elastic-perfectly plastic material and identical in tension and compression. Poisson's ratio of 0.3 and Elastic modulus, $E_s = 200,000\text{MPa}$ were used for steel reinforcement in this study, Fig. 8 shows the stress-strain relationship used in this study.

3.2.3 Epoxy

The behavior of the epoxy was assumed to be as that of concrete in tension.

4. ANALYTICAL METHODOLOGY

Fig.9 (a) and (b) show the volumes created in ANSYS and mesh of the concrete, steel plate, and reinforcement. Fig.10 show the boundary condition for supports and points of applied load.

5. NUMERICAL ANALYSIS AND COMPARISON OF RESULTS

5.1 First Crack Load

Table 2 liststhe experimental⁽²⁾ and FEM analysis values of first crack load , the experimental first crack obtained visually using a magnifying glass and the FEM first crack obtained from load steps.The first crack loads from FEM analysis and experimental data are within 9% for eight beams. In case one (control beam) the first crack load from ANSYS is higher than that from the experimental data by 16% , this is possibly due to the relative homogeneity of FEM model when compared to relative heterogeneity of actual beams that contain a number of micro-cracks. The FEM results also support the experimental observation in that after fixing the steel plate , the first crack load is agree with experimental data and the different is less than 8% in all six beams remained.

Also results show that the restraining effect of the glued plate on the appearance of first crack load is clear, using two plates glued at both sides of the flange is better in increasing cracking load than using only one plate with the same dimension at the middle of the beam, this might be due to the increase of the stiffness of the flange, which cracked first.

5.2 Ultimate Load

Table 3 compare the ultimate loads for full-size beams and the final loads from the finite element simulations. ANSYS underestimates the strength of beams by 1%- 10%. The first reason for the discrepancy is that the inclined portions of the steel reinforcement are excluded from the finite element models. Toughening mechanisms at the crack faces may also slightly extend the failures of the experimental beams before complete collapse. The finite element models do not have such mechanisms⁽⁷⁾.

Also Table 3 show the experimental, FEM and theoretical analysis values calculated according to the ultimate limit state simplified method of CP 110⁽⁸⁾ for all beams. The results show that generally the addition of the plates to the tested beams increased their ultimate loads. The maximum increase obtained was 157%, 153% and 155% (for experimental, FEM and theoretical analysis respectively), for beams strengthened with plate of b/t ratio 132.5.

While the maximum increase in the ultimate load of rectangular beams (120x200x2000mm dim) and (150x150x2300mm dim) studied by Abdel Hafez⁽⁹⁾ and Swamy et. al⁽¹⁰⁾ were 33% and 16% respectively. The results also shown that for the same dimensions of bonded plate, gluing two plates at the sides of the flange instead of one plate at the middle of the flange, reduced the ultimate capacity of the beam by about 13%, 17% (for experimental and FEM and respectively). From the values of ultimate load calculated according to method of CP 110⁽⁸⁾ given in Table 3 , it can be seen that this methods was under-estimate the ultimate load of most beams failed in flexure, while over-estimate of those failed in shear/bond.

5.3 Load Deflection Relationships

Figures 11 to 18 shown the typical load-deflection characteristics curves for the control and flexural strengthened beams for experimental⁽²⁾ and FEM results. Deflection is calculated at midspan at the center of the bottom face of the beams. In general, the load deflection curves for the beams from the FEM analyses agree quite well the experimental data. The finite element deflection curves in the linear range are somewhat stiffer than the experimental curves. After first cracking, the stiffness of finite element models is again higher than that of the experimental beams. There are several effects that may cause the higher stiffnesses in finite element models. First, microcracks are present in the concrete for the experimental beams, and could be produced by drying shrinkage in the concrete and/or handling of the beams. On the other hand, the finite element models do not include the microcraks. The microcraks reduce the stiffness of the experimental beams. Next, perfect bond between concrete steel reinforcing is assumed in the finite element analysis, but the assumption would not be true for the experimental beams. As bond slip occurs, the composite action between the concrete and steel reinforcing is lost. Thus, the overall stiffness of the experimental beams is expected to be lower than the finite element models (which also generally impose additional constrains on behavior).

Fig. 19 is an example show the distribution of deflection along the beam BA-4.

6. CRACK PATTERN

The ANSYS program records a crack pattern at each load step. Figures (20) and (21) shows the two samples of crack patterns developing for each beam at the last loading step. In general flexural cracks occur early at top of midspan as shown in Fig 20(a). When applied loads increase, vertical flexural cracks spread horizontally from the midspan to the support.

Increasing applied loads induces additional diagonal and flexural cracks, so at a higher applied load, diagonal tensile cracks appear as shown in Fig 20(b). Finally compressive cracks appear at nearly the last additional load step, Fig 20(c) shows the type of cracking signs observed for concrete elements underneath the loading.

Indeed no information obtained about the crack pattern of experimental beams. However, the cracks occur mostly in the high shear stress region. The crack pattern and steel yielding at mid span for the finite element Shear Beam support the experimental results that the beam fails in flexure as shown in Fig.21. Also the finite element model for beam BA-4 and BB-2 support the experimental beam failure as explained in crack pattern, the mode of failure in experimental beams is shear-bond failure as shown in Fig. 21, that is properly because the thickness of strengthened plate is high, i.e., b/t is small (31.75 and 58.33) for BA-4 and BB-2 respectively.

7. CONCLUSIONS

In this paper, nonlinear finite element analysis of plated T-beams subjected to negative bending moment comparison with experimental results and the following conclusions are drawn:

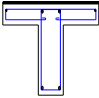
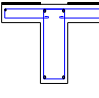
1. The proposed finite element model can be confidently used to predict the flexural behavior (deflection, cracking load and ultimate load) of either plated or conventional reinforced concrete beams.
2. The general behavior of the finite element models represented by load-deflection curves at midspan show good agreement with the test data from full-scale beam tests.
3. The final loads from the finite element analysis are lower than ultimate loads from the experimental results.
4. The addition of glued steel plates to the T-beams delays the appearance of the first visible crack, increase both the ultimate load and the flexuralstiffness, and improves the structural deformations of the beams at all load levels.
5. The maximum increase in the ultimate load over the unplated beam were 71%, 100%, 157% and 157% (66%, 105%, 153% and 149% in FEM) for beams strengthened with steel plates having the same cross sectional area and with b/t ratios equal 33.75, 58.33, 132.5 and 500 respectively .
6. The crack pattern and steel yielding at mid span for the finite element Shear Beam support the experimental results that the beam fails in flexure. Also the finite element

model agree well with the mode of failure in experimental beams that has a small b/t so it caused the failure in bond. The mode of failure is in shear-bond of two beams that is properly because the high thickness of strengthened plate.

REFERENCES

1. ANSYS 12.1 Finite Element Analysis System.
2. Zaid, S., Elrayes M. K., Abdel-Hafez, A. M. and Abdel-Hafez, L. M. 1997, "Experimental and Analytical Studies of Plated T-Beams Subjected to Negative Bending", ACI Structural Journal' Vol. 19, No.2, pp.873-878.
3. Desayi, P. and Krishnan, S., 1964, "Equation for the Stress-Strain Curve of Concrete", Journal for the American Concrete Institute, 61, pp.345-350, March.
4. Gere, J. M. and Tomoshenko, S. P., 1997, Mechanics of Materials, PWS Publishing Company, Boston, Massachusetts.
5. Wolanski A. J., 2004, "Flexural Behavior of Reinforced and Prestressed Concrete Beams using Finite Element Analysis", M.Sc. Thesis, University of Marquette.
6. Kachlakev, D. I. and Maccury, D.I., 2000, "Simulated Full Scale Testing of Reinforced Concrete Beams Strengthened with FRP Composite: Experimental Results and Design Model Verification" United State Department of Transportation, Fedral Highway Administration.
7. Shah, S. P., Swartz, S.E, and Ouyang, C., 1995, "Fracture Mechanics of Concrete", John Wiely& Sons, Inc., New York, New York.
8. BSI, , 1972, "British code of practice for the structural use of concrete" CP 110 Part1.
9. Magahed A., Abdul Hafez A. M. and Abdel Mageed M. A., 1991, "Flexural Behavior of R. C. Beams Strengthened" , Fourth Arab Structural Engineering Conference", Egypt, Nov, pp. 1-152-1-164.
10. Swamy R.N., Jones R., and Bloxham J. W., 1987, "Structural behavior of R.C. beams Strengthened by Epoxy Bonded Steel Plates", The Structural Engineering, V.65a, No.2, Feb., pp.59-68.
11. Gere, J. M. and Timoshenko, S. P., 1997, Mechanics of Materials, PWS Publishing Company, Boston Massachusetts.

Table (1): Details of Tested Beams.

Beam No.	Longitudinal reinforcing bars	Dimension of steel plate (mm)	* ¹ a/d ratio	* ² A _s bars (mm ²)	* ² A _s Plate (mm ²)	* ² A _s total (mm ²)	* ³ f _{cu} (Mpa)	Position of plate
BC-1	2 ϕ 13+ 2 ϕ 6	without	4.33	322	-	322	210	without
BC-2	6 ϕ 13+ 2 ϕ 6	without	4.33	852	-	852	230	without
BA-1	2 ϕ 13+ 2 ϕ 6	1x500	4.33	322	500	822	220	
BA-2	2 ϕ 13+ 2 ϕ 6	2x265	4.33	322	530	852	215	
BA-3	2 ϕ 13+ 2 ϕ 6	3x175	4.33	322	525	847	218	
BA-4	2 ϕ 13+ 2 ϕ 6	4x135	4.33	322	540	862	225	
BB-1	2 ϕ 13+ 2 ϕ 6	2(2x130)	4.33	322	530	852	218	
BB-2	2 ϕ 13+ 2 ϕ 6	2(3x87.5)	4.33	322	525	847	226	

*¹a/d : Shear span to effective depth ratio.

*²A_s: Sectional area of steel bars or plates

*³f_{cu}: Concrete compression strength measured by using cube 150x150x150mm.

Table (2): Comparison Between Experimental, FEM First Crack Load.

Beam No.	Dimension of steel plate (mm)	b/t*	First Crack Load (kN)		% Different
			Exp.	FEM	
BC-1	without	-	10	12	16%
BC-2	without	-	35	33	-6%
BA-1	1x500	500	35	32	-9%
BA-2	2x265	132.5	35	35	0%
BA-3	3x175	58.33	35	33	-6%
BA-4	4x135	31.75	42	38	-11%
BB-1	2(2x130)	130	42	38	-11%
BB-2	2(3x87.5)	58.33	42	38	-11%

*b/t – plate width to thickness ratio

Table (3): Comparison Between Experimental, FEM and Theoretical Results.

Beam No.	Dimension of steel plate (mm)	b/t*	Ultimate Load (kN)			<u>Exp</u> FEM	<u>Theo</u> FEM	Mode of failure
			Exp.	FEM	Theo.			
BC-1	without	-	49	47	39.7	1.04	0.84	flexure
BC-2	without	-	90	87.4	88.4	1.03	1.01	flexure
BA-1	1x500	500	126	117	96.7	1.08	0.82	flexure
BA-2	2x265	132.5	126	119	101.5	1.06	0.85	flexure
BA-3	3x175	58.33	98	96.7	101.2	1.01	1.05	flexure
BA-4	4x135	31.75	84	78	91	1.08	1.16	Shear/bond
BB-1	2(2x130)	130	112	97	101.5	1.10	1.05	flexure
BB-2	2(3x87.5)	58.33	84	81	101.2	1.04	1.20	Shear/bond

*b/t – plate width to thickness ratio

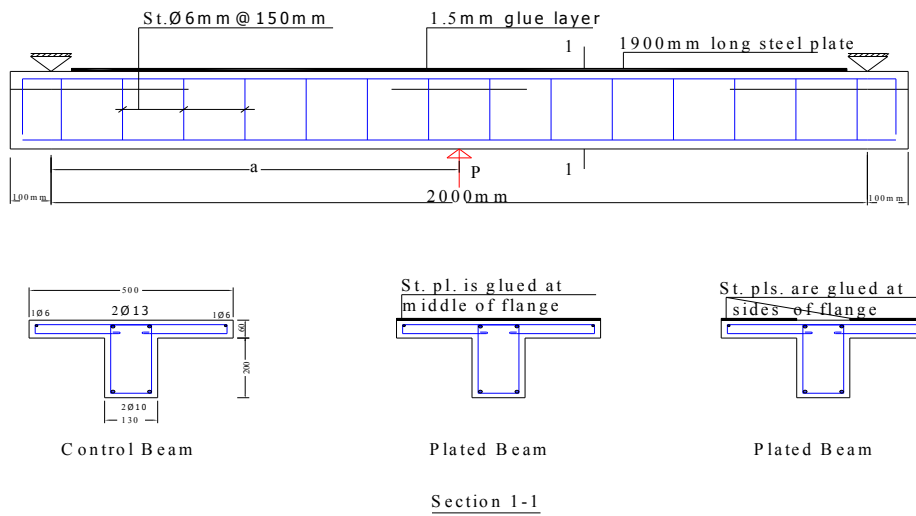


Fig.(1): Details of Tested Beams⁽²⁾

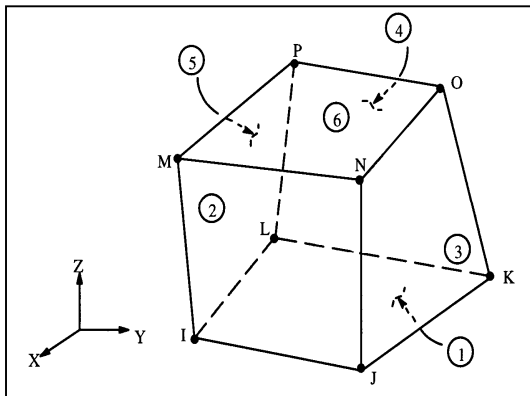


Fig.(2): Solid 65 Element.

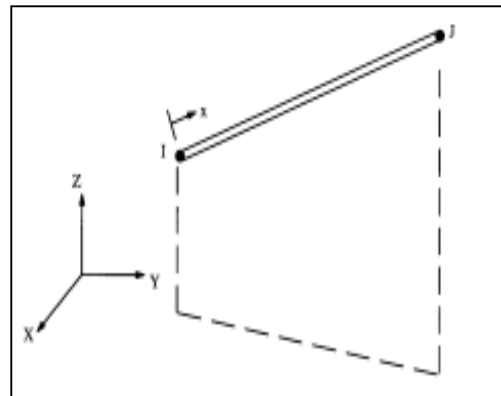


Fig.(3): Link8 Element.

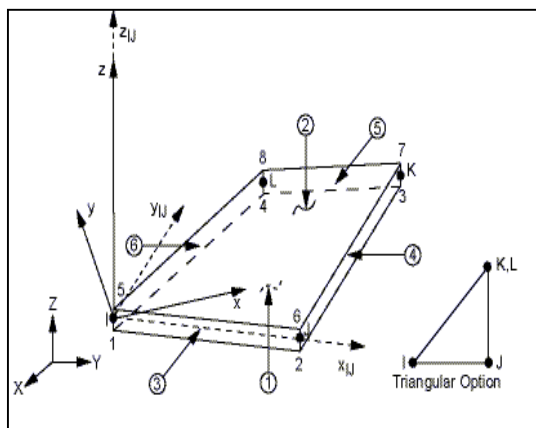


Fig.(4): Shell43 Element.

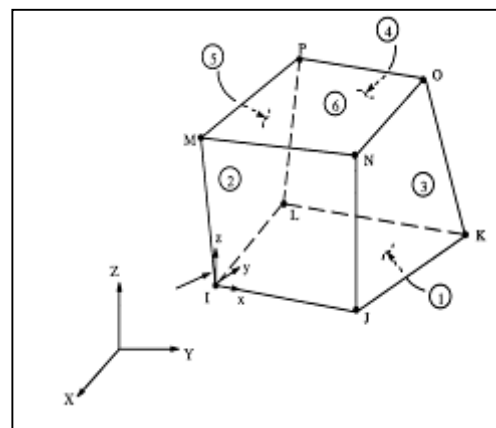


Fig.(5): Solid45 Element

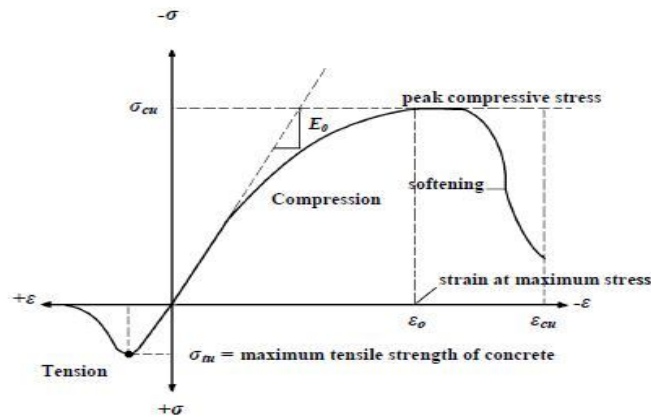


Fig.(6): Typical uniaxial compressive and tensile stress-strain curve of concrete.

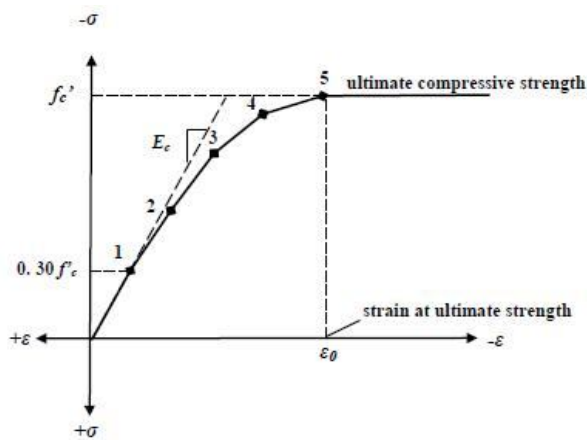


Fig.(7): Simplified compressive uniaxial stress-strain curve for concrete⁽⁷⁾

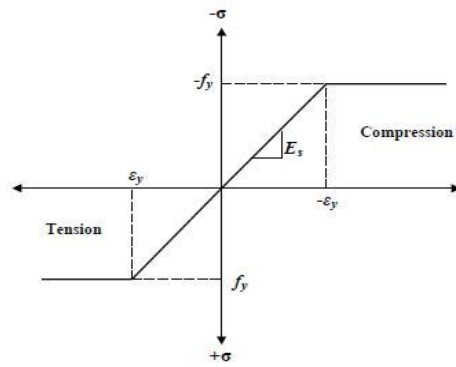


Fig.(8): Stress-strain curve for steel reinforcement.

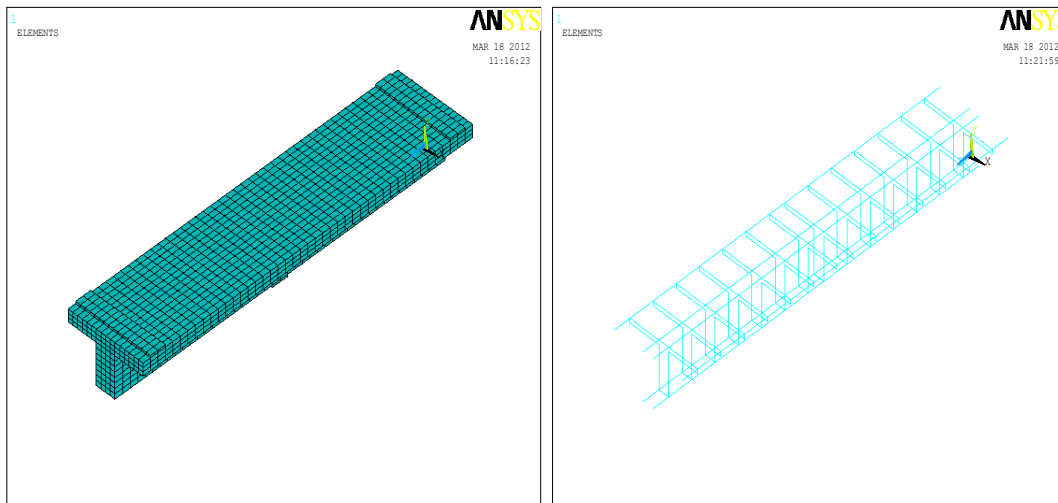


Fig.(9): (a) and (b) Volumes created in ANSYS and mesh of the concrete, steel plate, and reinforcement.

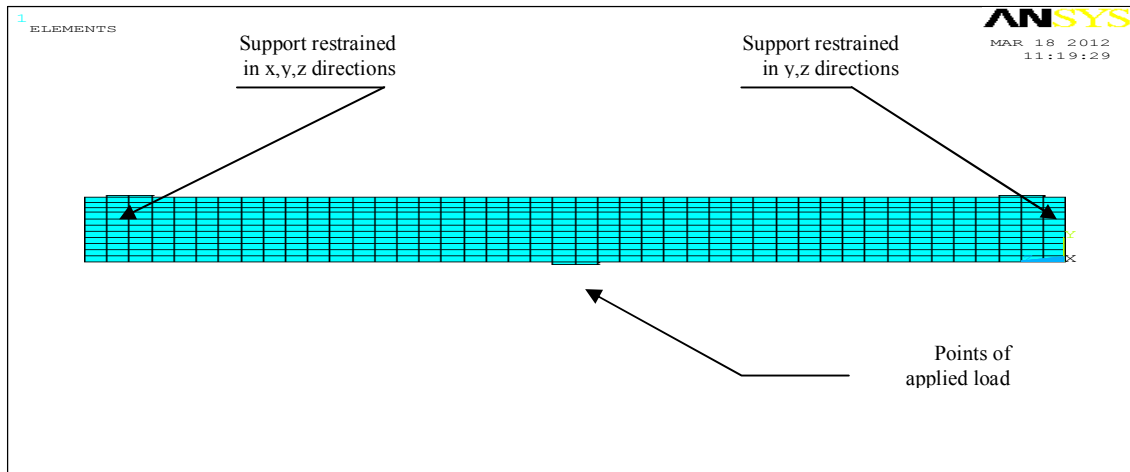


Fig.(10): Boundary condition for support and points of applied load

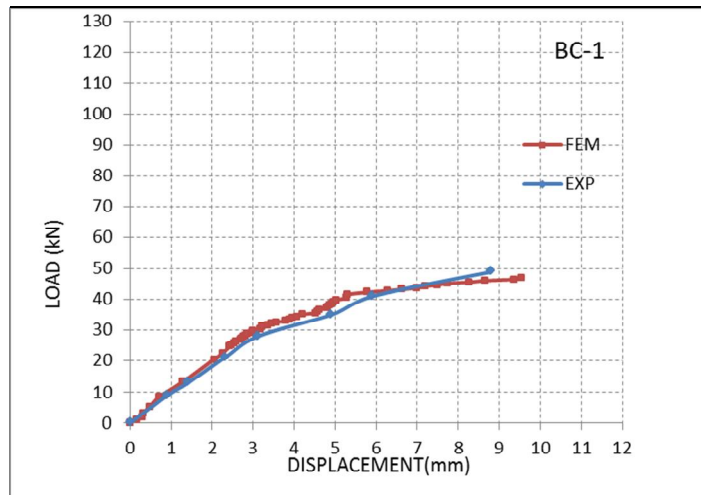


Fig.(11): Load-deflection curve of beam (BC-1).

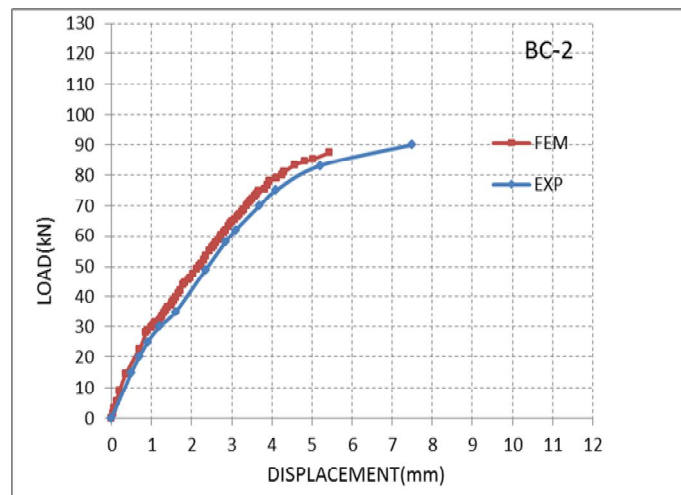


Fig.(12): Load-deflection curve of beam (BC-2).

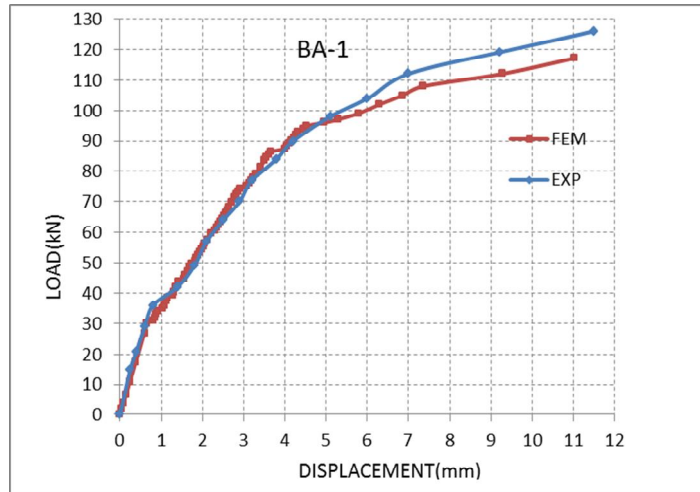


Fig.(13): Load-deflection curve of beam (BA-1).

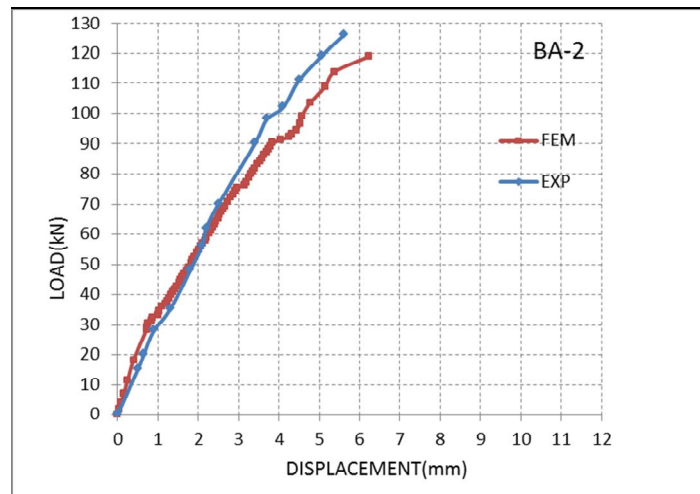


Fig.(14): Load-deflection curve of beam (BA-2).

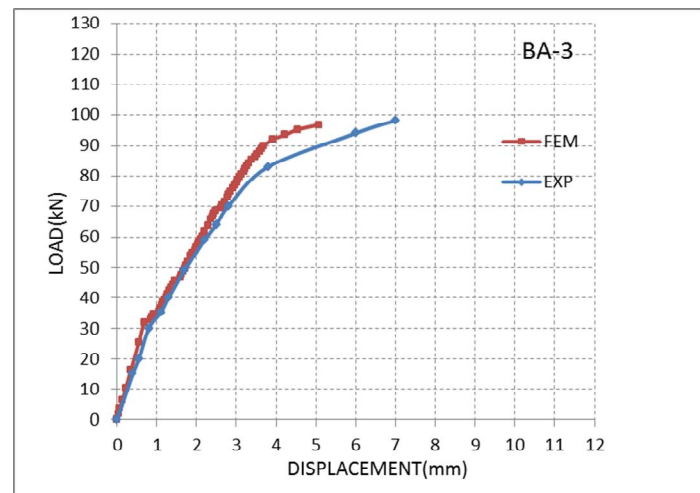


Fig.(15): Load-deflection curve of beam (BA-3).

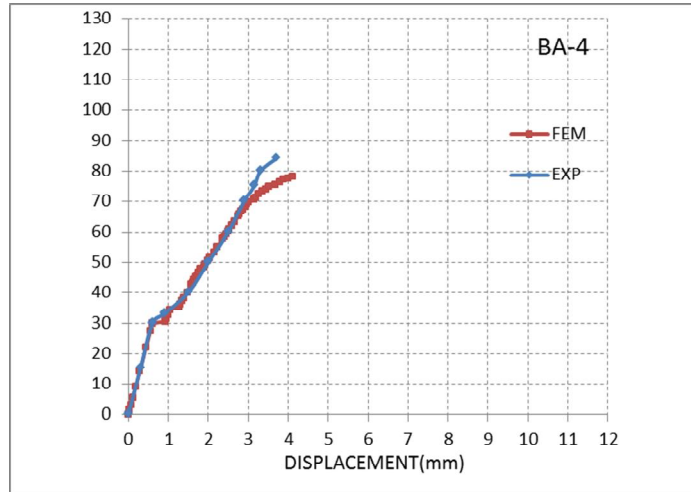


Fig.(16): Load-deflection curve of beam (BA-4).

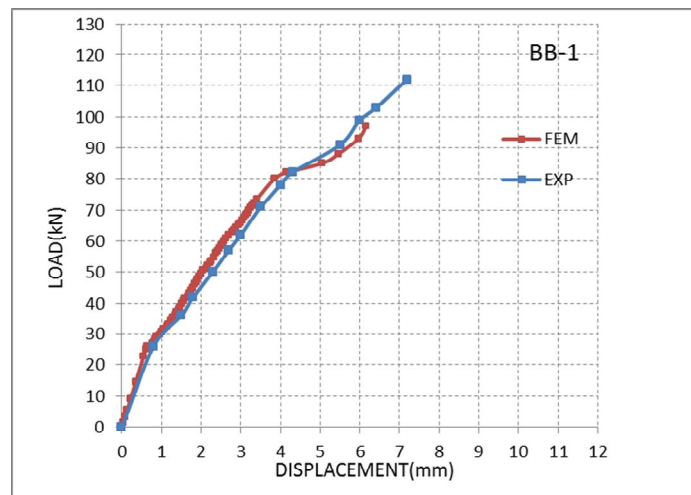


Fig.(17): Load-deflection curve of beam (BB-1).

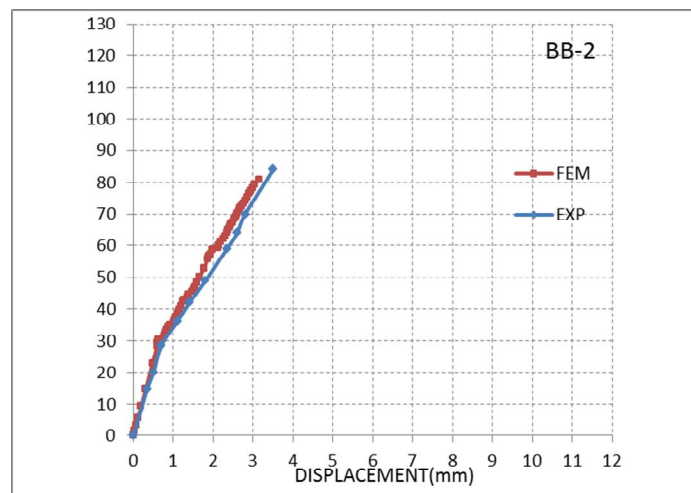


Fig.(18): Load-deflection curve of beam (BB-2).

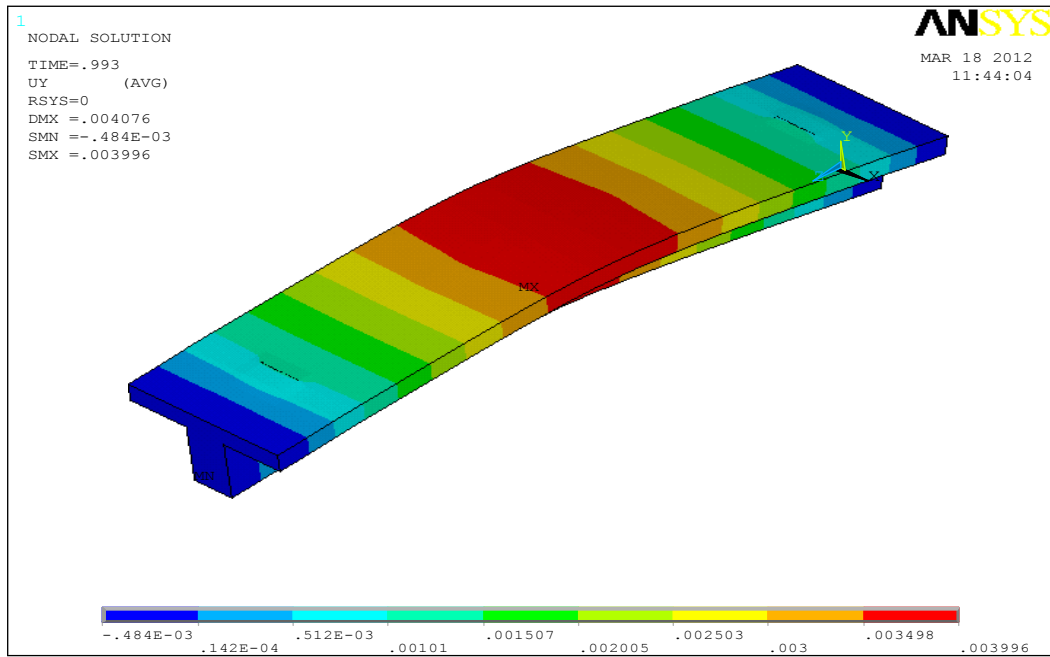


Fig.(19): Distribution of deflection along the beam BA-4.

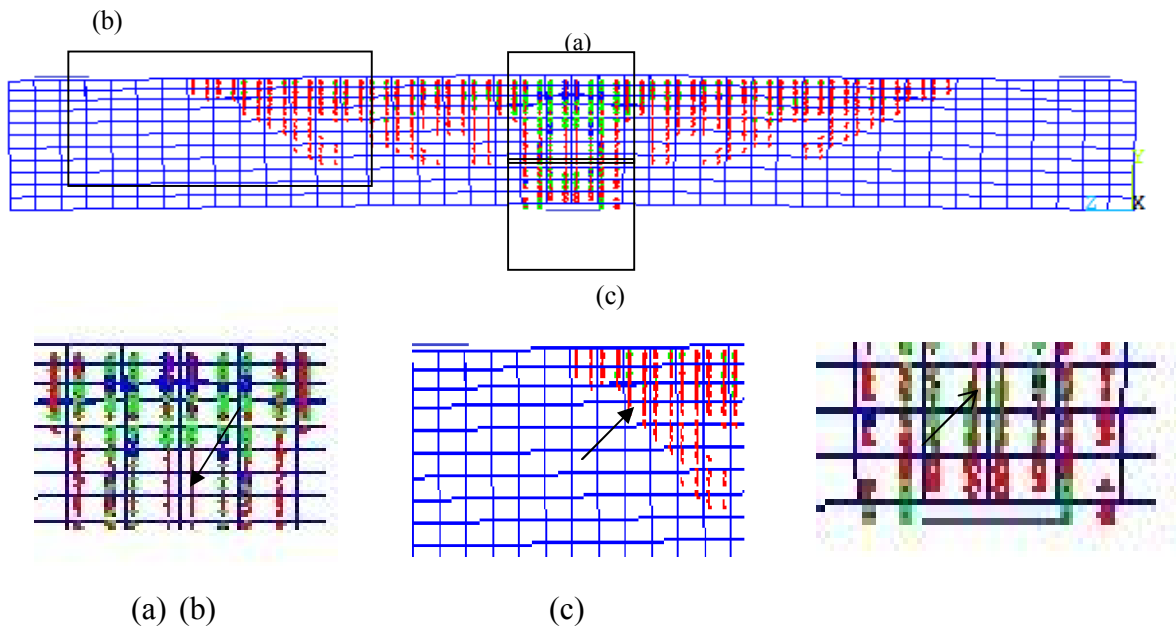


Fig. (20): Crack pattern of BC-1 (a) flexural cracks; (b) diagonal tensile cracks; (c) compressive cracks.

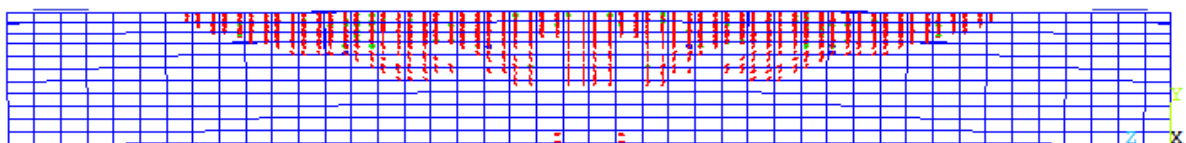


Fig. (21): Crack pattern of BB-2.

التحليل اللاخطي للعتبات المقواة بالبليت ذات مقطع T والموضوعة تحت تأثير الانحناء السالب

منصور عبدالله احمد

مدرس مساعد

كلية الهندسة- جامعة ديالى

الخلاصة

يتضمن البحث استخدام برنامج ANSYS لتمثيل و تحليل (لا خطي) لعتبات ذات مقطع T مقواه ببليت من الحديد للأجزاء المعرضة الى انحناء سالب (أي أن التحميل من أسفل العتبة). جميع العتبات كانت بطول ٢متر ومسندة أسناد بسيط ومحملة تحميلا مركزيا في وسط العتبة. تم اعتماد نتائج بحوث عملية لثمانية نماذج من العتبات^(١) ، وقد تم تمثيل المواد (الخرسانة، حديد التسليح، البليت) وتصرفها اللاخطي من خلال عمل الموديل الملائم لها في البرنامج. نتائج التحليل بواسطة برنامج ANSYS أظهرت أن التصرف العام لموديل العتبات والمتمثلة بعلاقة التحميل- الانحراف في وسط العتبة يتطابق بشكل جيد مع نتائج الفحوصات العملية. إضافة الى ذلك تم مناقشة شكل التشققات في المرحلة النهائية للتحميل في موديل العتبات. نتائج هذا البحث باستخدام برنامج ANSYS يمكن أن تستخدم لعمل دراسة قياسية عن العتبات ذات مقطع T مقواه ببليت من الحديد.